Magnitude limited age distribution of a synthetic O and B star population

Andreas Müller

Bachelorarbeit in Physik
angefertigt im Argelander Institut für Astronomie

vorgelegt der
Mathematisch-Naturwissenschaftlichen Fakultät
der
Rheinischen Friedrich-Wilhelms-Universität
Bonn

Mai 2015

Ich versichere, dass ich diese Arbeit selbstständig verfasst und keine anderen als die angegebenen Quellen und Hilfsmittel benutzt sowie die Zitate kenntlich gemacht habe.

Bonn, ...

Datum Unterschrift

1. Gutachter: Prof. Dr. Norbert Langer
2. Gutachter: PD. Dr. Thomas Tauris

Contents

CHAPTER 1

Introduction

Magnetic fields in massive stars play a major role in their evolution, yet the origin and development of those fields is still an unsolved puzzle [1]. While large scale surface magnetic fields seem to be ubiquitous in low mass stars on the main sequence, in intermediate-mass stars only a fraction of 10%, the chemically peculiar, show such a field [2] with the rest hosting, if any, very weak large-scale fields. We know that about 7% of massive main sequence stars show a measurable large-scale magnetic field [3]. Except for magnetic braking [4] the impact of these fields on the evolution of massive stars is largely unknown [5].

In a paper by Fossati et al. (2015 in prep.) it is proposed, that some massive stars start out with a strong magnetic field that, in most cases, decays over the main sequence lifetime of the star. In mapping the probability density for massive magnetic main sequence stars with apparent visual magnitudes $V < 9$ as a function of fractional main sequence age (τ), Fossati et al. made an unexpected observation. The probability density for those massive magnetic stars is not a monotonically decreasing function, but peaks once at low τ before declining. This is caused by the fact that the probability density for all measured magnetic and non-magnetic galactic main sequence O and B stars increases with fractional main sequence age (τ) (figure 1.1).

Either there is an intrinsic age distribution in galactic O and B stars, or there is an observational bias towards stars of higher τ. Our proposed explanation is that because stars become more luminous as they age, we see more old stars than young ones.

In this thesis I simulate a synthetic stellar population to determine whether the observed trend in figure 1.1 is due to the applied magnitude limit or rather due to an intrinsic age distribution that favours older stars. In section 2.1 a probability density function (PDF) of all stars with respect to τ is determined. Using the analytical formulations by Hurley et al. (2000) [6] in section 2.2 the apparent visual magnitude of every star in the population is computed. A few tests are run and corrections are made in section 3. In section 4 the PDF of all stars below the the magnitude limit is compared to the distribution from figure 1.1. Finally these results are discussed and conclusions are drawn in section 5.

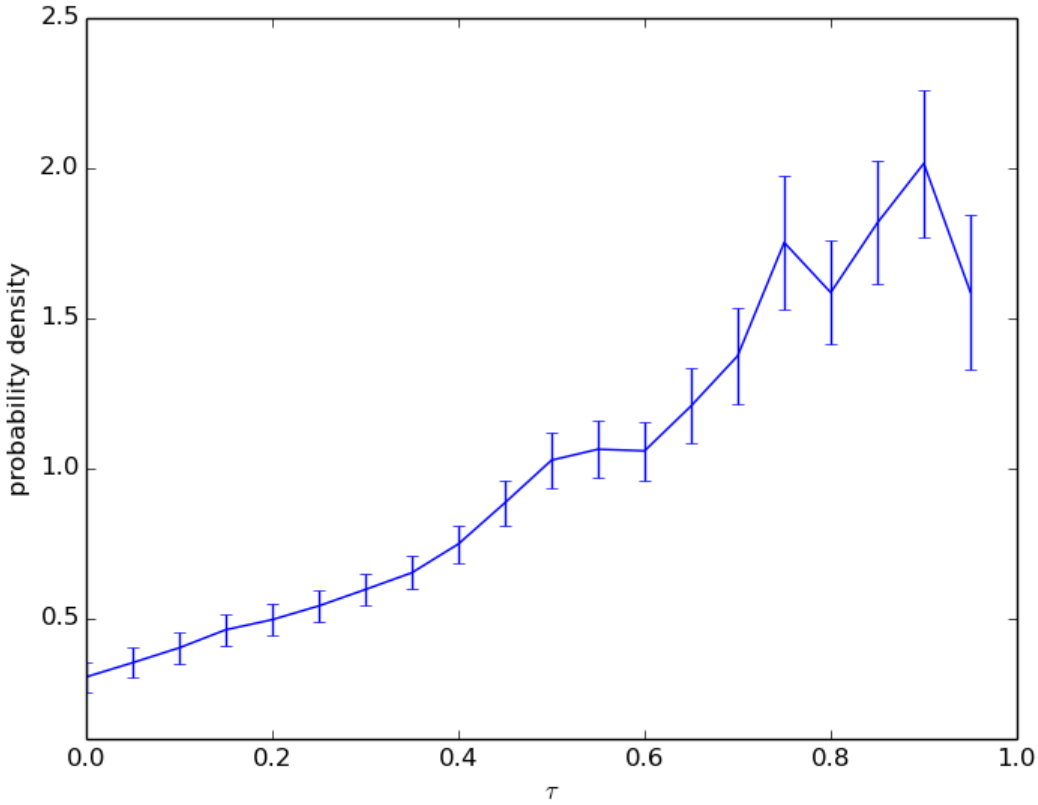

Figure 1.1: Probability density of galactic O and B stars with apparent visual magnitudes $V < 9$ as a function of fractional main sequence age with error bars. Data taken from Fossati et al. (2015 in prep.)

CHAPTER 2

Method

2.1 Simulating a stellar population

The stars in my synthetic stellar population are characterized by three parameters: distance from earth (r), stellar mass (M) and age (t). In accordance to the observational data that I model, distance ranges from 0 to $r_{\max} = 3\,\mathrm{kpc}$ and mass from $M_{\min} = 5\,\mathrm{M}_\odot$ to $M_{\max} = 50\,\mathrm{M}_\odot$. Because the main sequence lifetime (t_{ms}) of a star is a monotonically increasing function of mass, the age of the oldest, i.e. the least massive star with mass $M_{\min}$, in the population is $t_{\max} = t_{\mathrm{ms}}(M_{\min})$. For $M_{\min} = 5\,\mathrm{M}_\odot$ and using the fitting formula for main-sequence lifetime of Hurley et al. (2000) [6, equation 5] this translates to $t_{\max} \approx 104\,\mathrm{Myr}$.

I formulate a probability density in fractional main sequence age ($\frac{dp}{d\tau}$) using the probability densities for stars in space $\left(\frac{dp}{dV}\right)$, mass $\left(\frac{dp}{dm}\right)$ and age $\left(\frac{dp}{dt}\right)$. In my simulation I assume that the stars are uniformly distributed in space. Because of the radial symmetry of the problem, the distribution is solely dependent on the distance from earth, i.e.

$$\frac{dp}{dV} = \frac{1}{V_{\mathrm{tot}}} = \frac{1}{\frac{4}{3}\pi r_{\max}^3}. \tag{2.1}$$

I assume that the stars are distributed in mass according to the Salpeter initial mass function (IMF); $\frac{dp}{dM} = A \cdot M^{-2.35}$ [7]. Because the IMF follows an inverse power law, I use a logarithmic binning in mass. Because of that I need to convert the IMF to a logarithmic formulation using $d\log M = \frac{dM}{M \ln 10}$

$$\frac{dp}{d\log M} = \ln 10 \cdot A \cdot M^{-1.35}, \tag{2.2}$$

where A is a normalization factor, that follows from

$$1 = \int_{M_{\min}}^{M_{\max}} A \cdot M^{-2.35} dM = \left[\frac{1}{-1.35} \cdot A \cdot M^{-1.35}\right]_{M_{\min}}^{M_{\max}}, \tag{2.3}$$

$$A = \frac{1.35}{M_{\min}^{-1.35} - M_{\max}^{-1.35}}. \tag{2.4}$$

I assume a constant star formation rate, so the probability density in age is $\frac{dp}{dt} = \frac{1}{t_{\mathrm{ms}}}$. The age axis is also defined logarithmic to make sure massive stars with small t_{ms} are correctly represented. Because of this I need to find $\frac{dp}{d\log t}$ using $d\log t = \frac{dt}{t \ln 10}$, i.e.

$$\frac{dp}{d\log t} = \frac{t \ln 10}{t_{\mathrm{ms}}}. \tag{2.5}$$

With this information I can formulate the overall probability density function (PDF) for the stars in my sample with regard to τ

$$\frac{dp}{d\tau} = \frac{dp}{dV}dV \cdot \frac{dp}{d\log t}d\log t \cdot \frac{dp}{d\log M}d\log M \cdot \frac{1}{d\tau}. \tag{2.6}$$

2.2 Apparent visual magnitude

The first step I made towards finding the apparent visual magnitude (V) of a star is to use analytical fitting formulas by Hurley et al. (2000) [6] which approximate the stellar radius (R) and luminosity (L) as a function of initial mass (M_{ini}), fractional main sequence age (τ) and metalicity (Z). From equation 5 from that paper I obtain the main sequence age for any given stellar mass $t_{\mathrm{ms}}(M)$ and τ then becomes: $\tau(M) = \frac{t}{t_{\mathrm{ms}}(M)}$. I use Z=0.02 for all stars to simulate a metalicity similar to that of our sun according to Grevesse & Sauval (1998) [8]. I then use Equation 12 and 13 from Hurley et al. (2000) to compute luminosity (L) and radius (R) for stars on the main sequence[1].

Figure 2.1 shows a Hertzsprung-Russel diagram (HRD) for six different stars on their main sequence based on the fitting formulas by Hurley et al. (2000). To obtain the effective temperature (T_{eff}) I use the following equation with σ being the Stefan-Boltzmann-Constant:

$$T_{\mathrm{eff}} = \sqrt[4]{L/(\sigma 4\pi R^2)}. \tag{2.7}$$

Knowing distance, mass, age, fractional main sequence age, luminosity and radius I can compute the apparent visual magnitudes using the following equations:

$$M_{\mathrm{V}} = V - 5 \cdot \log(r) + 5 - A(r), \tag{2.8}$$

$$M_{\mathrm{bol}} = M_{\mathrm{V}} + BC(T_{\mathrm{eff}}), \tag{2.9}$$

$$\log(L/\mathrm{L}_{\odot}) = 0.4 \cdot (4.72 - M_{\mathrm{bol}}). \tag{2.10}$$

M_{V} is the absolute visual magnitude, $\log(r)$ is the logarithm to base ten of the distance from earth. $A(r)$ is the reddening and M_{bol} is the absolute bolometric magnitude. $BC(T_{\mathrm{eff}})$ is the bolometric correction as a function of the effective temperature T_{eff} (see equation 2.7) by Flower (1996) [10]. Using equations 2.8, 2.9 and 2.10 I can compute the apparent visual magnitude V:

$$V = 5 \cdot \log(r) - 0.28 + A(r) - \frac{\log(L/\mathrm{L}_{\odot})}{0.4} - BC(T_{\mathrm{eff}}). \tag{2.11}$$

To get a rough approximation for reddening, I use Amôres & Lépine (2005) [11, Figure 9]. I linearly interpolate the three intervals between $r = 0\,\mathrm{kpc}$ and $A = 0$, $r = 1\,\mathrm{kpc}$ and $A = 0.9$, $r = 2\,\mathrm{kpc}$ and $A = 2.25$, $r = 3\,\mathrm{kpc}$ and $A = 3.27$.

[1] Hurley et al. (2000) [6] cite Tout et al. (1996) [9] for zero age main sequence radii and luminosities. In Equation 1 of Tout et al. (1996) there is a typo. Instead of $\gamma + M^3$ it should read $\gamma \cdot M^3$.

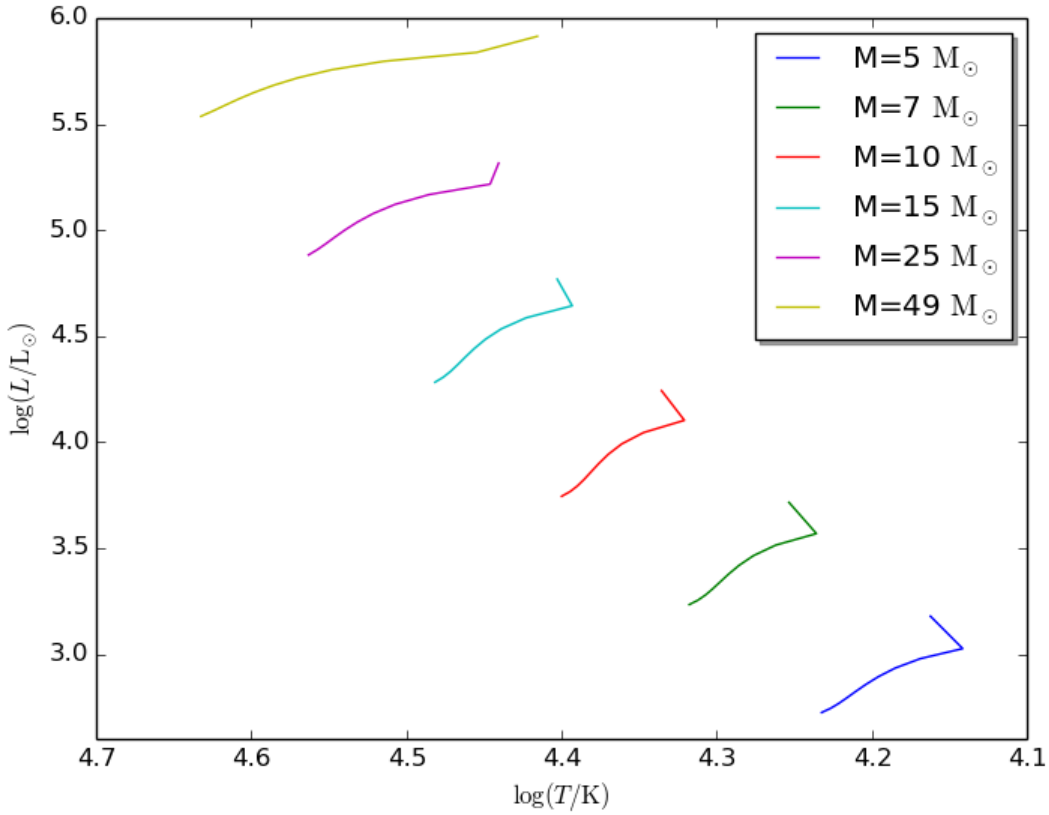

Figure 2.1: HRD for six different stars on their main sequence based on analytical fitting formulas by Hurley et al. (2000)[6]

CHAPTER 3

Consistency and numerical tests

I run a few consistency and numerical tests: In section 3.1 the reddening model I use will be evaluated and some corrections will be made. In section 3.2 the fact, that I used a different evolutionary model for my simulation than the one the observational data is evaluated with will be discussed and effects of this will be shown. In section 3.3 the resolution I use in computing the final data will be deduced.

3.1 Reddening model

Figure 3.1 shows the difference between computed and observed magnitude for a sample of 150 O and B stars from Castro et al. (2014) [12] as a function of logarithmic distance. The theoretical magnitudes (V_{comp}) were computed using stellar radius, luminosity, distance and equation 2.11. All observational data is taken from a sample by Castro et al. (2014) which is infered from analytical fitting formulas by Brott et al. (2011) [13]

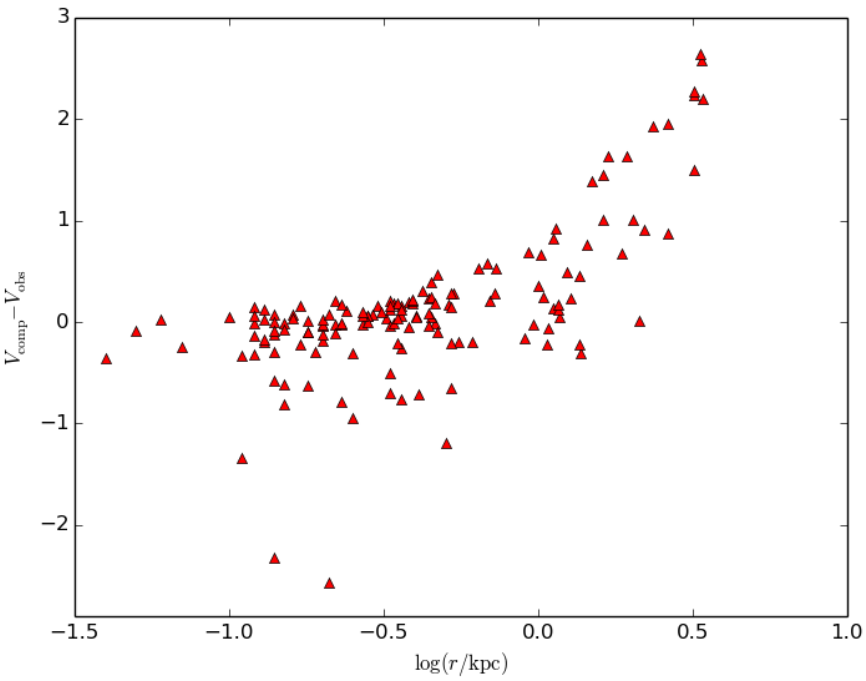

Figure 3.1: Difference between computed and observed magnitude as a function of $\log(r/\mathrm{kpc})$.

There is a smooth increase of $V_{\text{comp}} - V_{\text{obs}}$ with distance. This is caused by the fact that the reddening model I use is averaged over the entire sky. Because of dense pockets of gas and dust the actual extinction can deviate a lot from the average. Some areas are extremely obscured and stars in these areas may fall below V=9 thus making the star not part of my sample. These areas do however contribute to the average reddening, making my reddening function too steep [11]. To correct this I introduce a new reddening function $A'(r) = 0.3 \cdot A(r)$. Figure 3.2 shows the same graph as figure 3.1 with this correction.

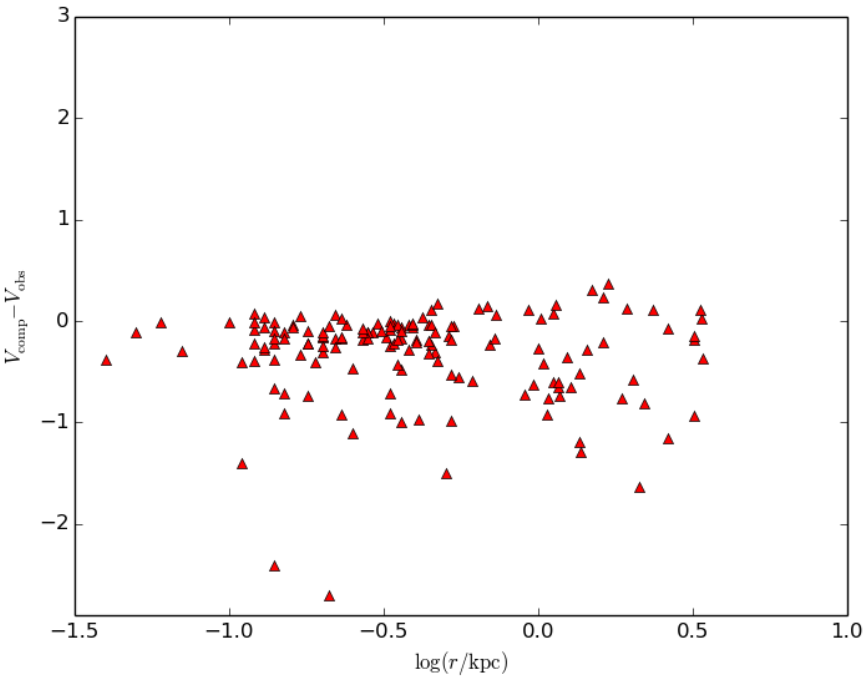

Figure 3.2: Same as figure 3.1 using the modified reddening function $A'(r)$.

With the adjusted reddening function, the observed and computed magnitudes still don't match. There remains a tendency to negative values caused by extinction. As seen in figure 3.3 it is most prevalent in the youngest stars. Young stars are primarily found in regions of high gas density. This gas causes extinction and thus increase V_{obs}. As explained above, my extinction model is an approximation that is averaged over the entire sky and does not take into account these density fluctuations.

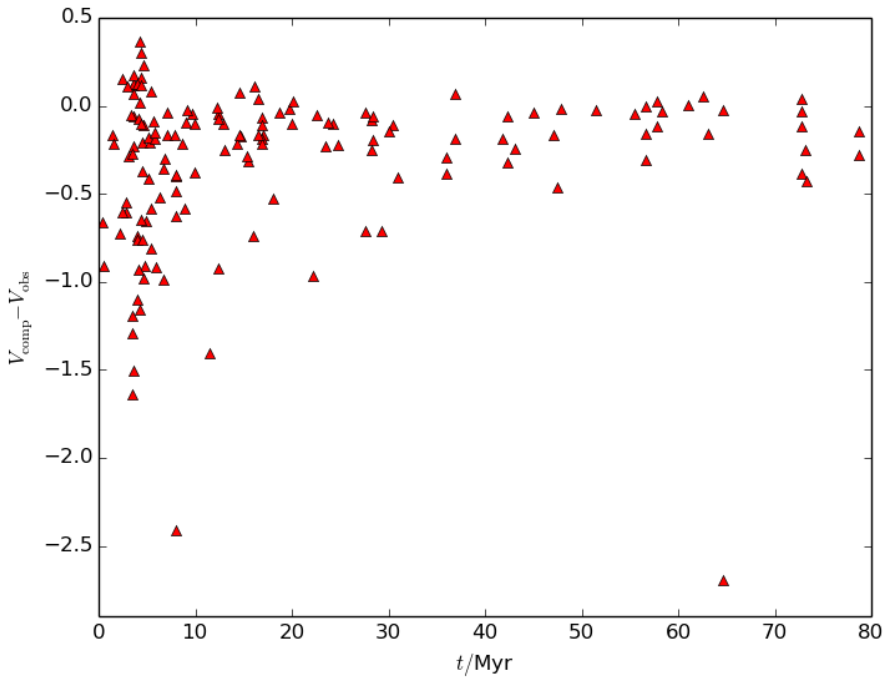

Figure 3.3: Difference between computed and observed magnitude as a function of age using $A'(r)$.

3.2 Evolutionary model

The observational data is processed using a stellar evolution model by Brott et al. (2011) [13], whereas I used fitting formulas by Hurley et al. (2000) [6], which are based on a model by Pols et al. (1998) [14]. To quantify the differences due to this fact, for every one of the 150 stars used in section 3.1 I compute the visual magnitudes using the luminosity and stellar radius infered from the model by Brott et al. (2011) ($R_{\rm Brott}$, $L_{\rm Brott}$) and compare them to the visual magnitudes computed with the fitting formulas by Hurley et al. (2000) using mass (M) and fractional main sequence age (τ).[2]

I use M and τ to compute $\log(L/\mathrm{L}_\odot)_{\rm Pols}$ and $\log(R/\mathrm{R}_\odot)_{\rm Pols}$ using the fitting formulas based on Pols et al. (1998). Figure 3.4 shows that the main difference in these two models originates in the differing radii. The top panels and the bottom left panel show the same trend where the radius and subsequently the effective temperature and the visual magnitudes differ strongly at terminal age main sequence (TAMS). As seen in the bottom right panel this is only the case in stars of masses above $M = 20\,\mathrm{M}_\odot$

These trends originate in the fact, that the model by Brott et al. (2011) takes into account inflation whereas the model by Pols et al. (1998) does not. Near TAMS on the main sequence massive stars undergo an inflation of their envelopes. Because the luminosity of these stars does not change much, the temperature subsequently drops as seen when comparing the top two panels of figure 3.4. This shifts the peak of their planck-distribution to lower wavelengths and gives rise to a systematic error in the bolometric correction and subsequently in their visual magnitudes.

[2] mass and fractional main sequence age are infered from the stellar evolution model by Brott et al. (2011) [13].

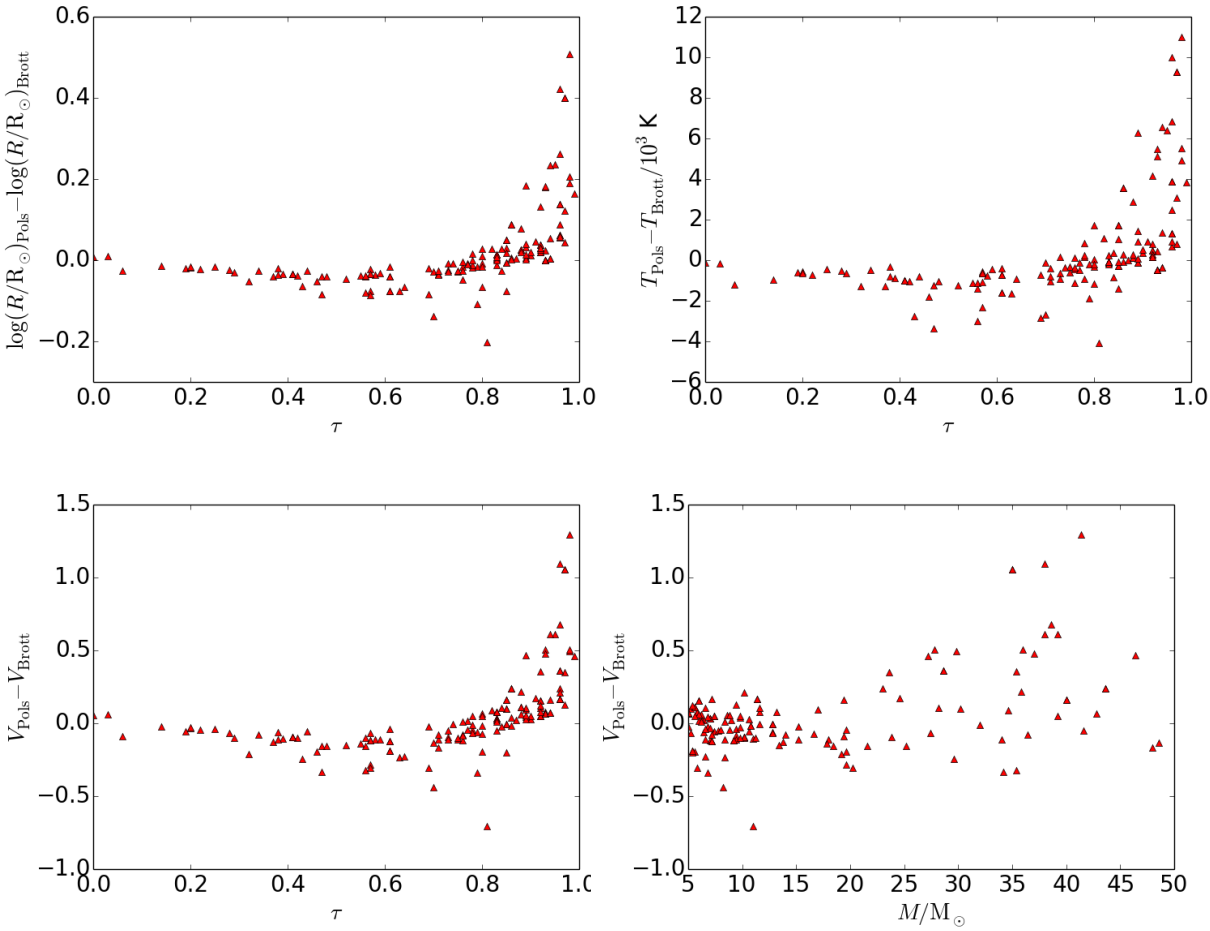

Figure 3.4: Four graphs comparing the stellar evolution models by Pols et al. (1998) and Brott et al. (2011). The top two graphs show the difference in logarithmic radii (left) and the effective temperatures (right) as a function of fractional main sequence age and the bottom graphs show the difference between visual magnitudes as a function of fractional main sequence age (left) and stellar mass (right).

3.3 Resolution

To minimize computing time and maximize accuracy, I deduce an appropriate binning for each of the three variables, that characterize the stars in my population. Figure 3.5 shows the PDF for all stars in my sample with a magnitude cut at V=9 in four graphs. The upper left panel shows both the function with a binning in distance-mass-age of 100-100-100 and the final results without noise for reference. One can see from this panel that there is still noise that needs to be eliminated. To understand what variables play the biggest role in creating this noise, in the other panels I reduce the resolution of one select variable and compare the resulting curve to the curve of 100-100-100 resolution.

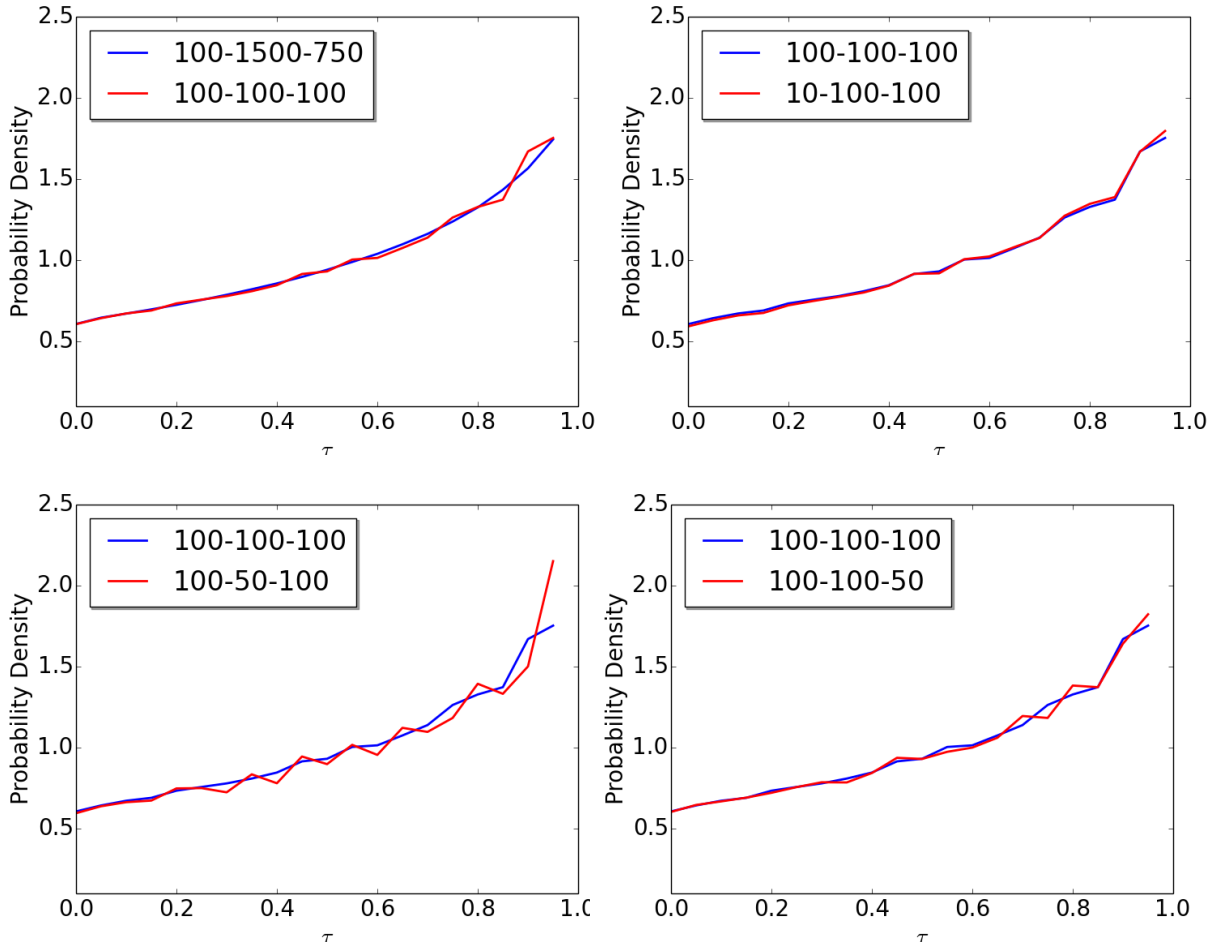

Figure 3.5: PDF for all stars in my sample with a magnitude cut at V=9 with different binnings. The legend is to be read as follows: The first value is the binnig in distance, the second is mass and the third is age.

In the upper right panel of figure 3.5 one can see that even though I reduce the resolution of distance by one order of magnitude, the curves only deviate very little. This tells me that distance is robust to a low resolution. The bottom panels, even though I only reduced the resolution by a factor of two, both show a significant increase in noise, the bottom left panel showing the greatest deviation from the reference-curve. Using these results, I determine a resolution of 100-1500-750 to maximize accuracy and minimize computing time.

CHAPTER 4

Results

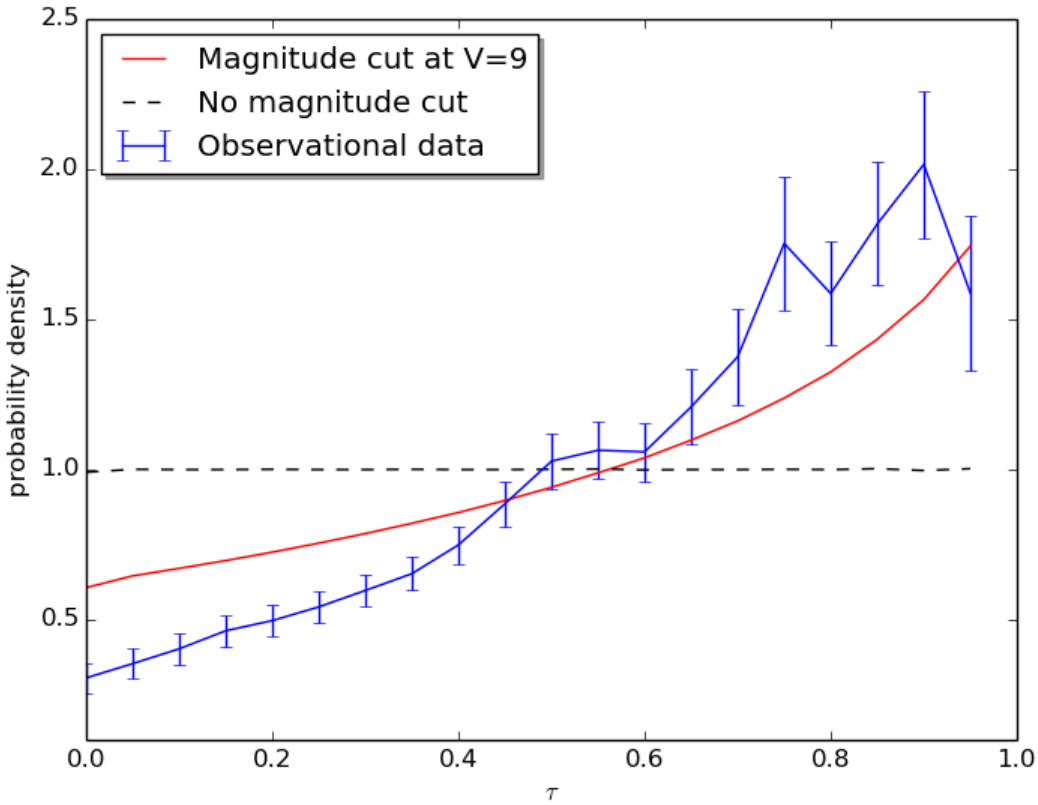

Figure 4.1: PDF of a volume limited sample with magnitude cut at V=9 (red line), without magnitude cut (dashed line) and observational data with error bars (blue line). The observational data is taken from Fossati et al., (in prep.).

Figure 4.1 shows the PDF of all stars in the volume limited sample with magnitude cut at V=9, the PDF without magnitude cut and observational data with error bars. The PDF without magnitude cut shows that the stars are uniformly distributed in τ. This was expected, because I assumed a constant star formation rate in the simulation. It confirms, that the slope of the red curve is entirely due to the magnitude cut.

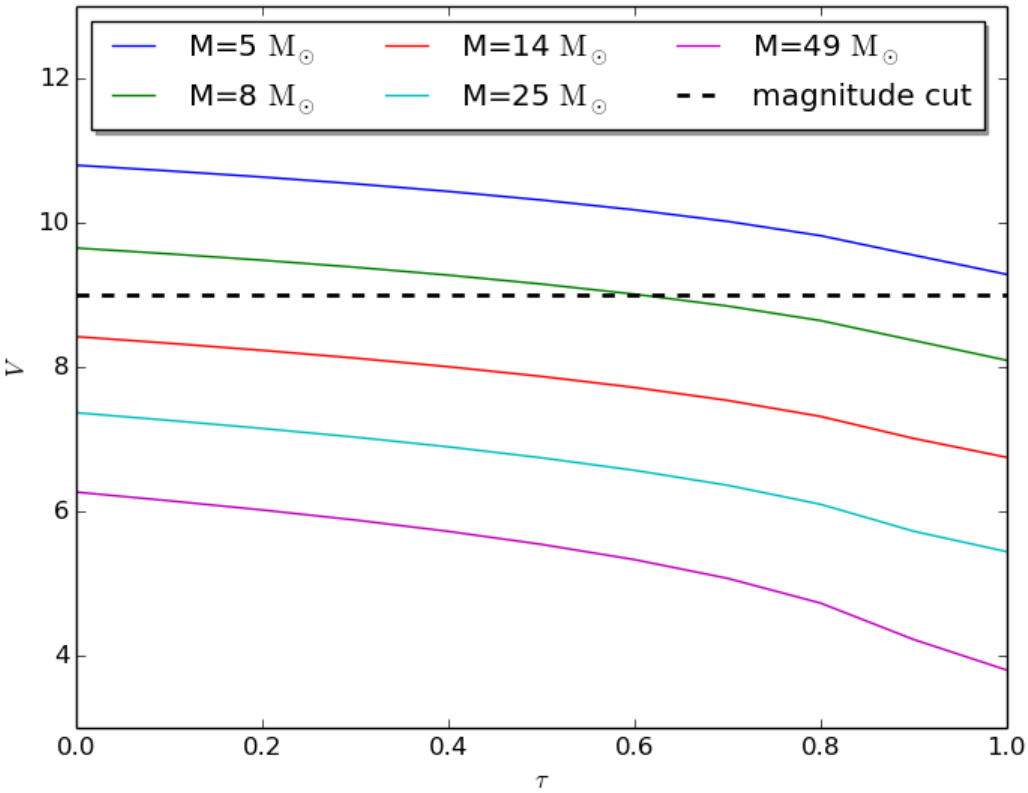

Figure 4.2: V as a function of fractional main sequence age for five different stars at a distance of 1.5 kpc based on analytical formulations by Hurley et al. (2000) [6] The dashed line shows the applied magnitude cut.

Introducing a magnitude cut produces a similar trend to the one observed in the observational data. Because V is a monotonically decreasing function of age, there are more old stars below the magnitude cut than young stars. Figure 4.2 shows V as a function of τ for five different stars at a distance of 1.5 kpc based on the analytical fitting formulas by Hurley et al. (2000) [6]. One can observe how stars that start their lives above the magnitude cut evolve to become more luminous and cross the magnitude cut during their evolution (see the $M = 8\,\mathrm{M}_\odot$ model).

Even though the computed curve does have a similar trend to the observations, it needs to be explained why the curve is not as steep. A slope too shallow may indicate an intrinsic age distribution of galactic stars. I will present some possible improvements in section 5.

CHAPTER 5

Discussions and conclusions

In a magnitude limited survey of galactic O and B stars, one observes an increasing probability density with increasing fractional main sequence age (figure 1.1). To understand this trend I set up a synthetic stellar population of stars on their main sequence with masses between $M = 5\,\mathrm{M}_\odot$ and $M = 50\,\mathrm{M}_\odot$ in a sphere of radius $r_{\mathrm{max}} = 3\,\mathrm{kpc}$. I defined the probability density function (PDF) with regard to the fractional main sequence age $\frac{dp}{d\tau}$ and implemented analytical formulations by Hurley et al. (2000) [6] to find the apparent visual magnitude of every star in the sample. With this information I was able to plot the magnitude limited PDF and compare it to the observational data (Figure 4.1).

I was able to reproduce the trend of the observational data to a good degree and found strong arguments for our initial hypothesis that this trend appears due to observational bias. It needs to be explained however, why the slope of the computed PDF is more shallow than the slope of the observed curve.

In the future my work can be used to simulate a more detailed model of stellar population and reduce the deviations that occur in this simulation. There are five major things, that can be improved upon:

- The reddening model is an approximation, that does not take into account density fluctuations in the interstellar medium. I had to implement a correction factor to eliminate a systematic error. In the future implementing a more detailed reddening model will be integral.
- To obtain the data presented in figure 1.1 a different stellar evolution model (Brott et al., 2011) [13] was used , than the one on which the fitting formulas by Hurley et al. (2000) [6] are based. This results in systematic uncertainties. In the future this should be avoided.
- The stars are distributed homogeneously in a sphere of 3 kpc radius. Since the galactic disk however has a thickness of about 200pc. The probability density in volume has to be adjusted accordingly (equation 2.1).
- My model does not take into account binary stars. This possibly has a great effect on the population because binary interactions play a major role in the evolution of most massive stars with only about 30% being effectively single [15].
- We know from observations that we live in a part of the galaxy with little star formation. As seen in figure 5.1 the density of young open star clusters increases the farther they are away from the solar system. One could implement a star formation history reflecting that, introducing a distance-dependancy in equation 2.5.

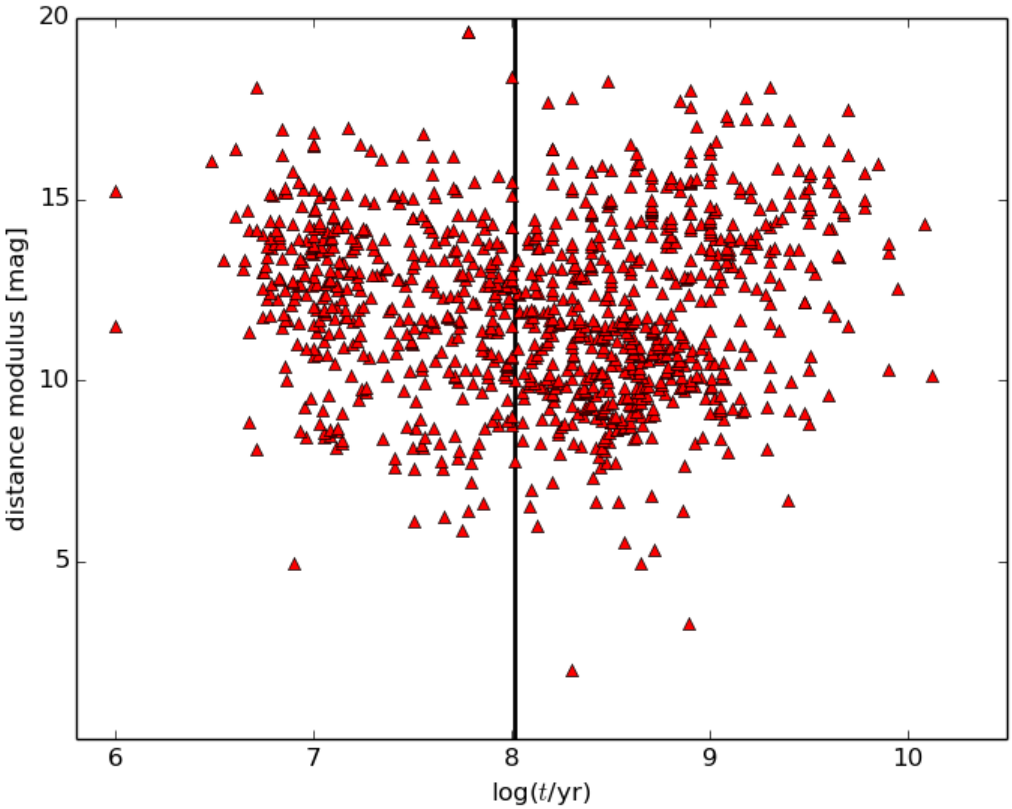

Figure 5.1: Open star clusters in our galaxy with distance modulus vs logarithmic age. The black line represents the age of the oldest possible star in my synthetic population. ($t_{\mathrm{ms}}(M_{\mathrm{min}}) = 104\,\mathrm{Myr}$) [16]

Bibliography

[1] N. Langer, *Presupernova Evolution of Massive Single and Binary Stars*, ARA&A **50** (2012) 107–164, arXiv: 1206.5443 [astro-ph.SR] (cit. on p. 1).

[2] J.-F. Donati and J. D. Landstreet, *Magnetic Fields of Nondegenerate Stars*, ARA&A **47** (2009) 333–370, arXiv: 0904.1938 [astro-ph.SR] (cit. on p. 1).

[3] G. A. Wade et al., "The magnetic characteristics of Galactic OB stars from the MiMeS survey of magnetism in massive stars", *IAU Symposium*, vol. 302, IAU Symposium, 2014 265–269, arXiv: 1310.3965 [astro-ph.SR] (cit. on p. 1).

[4] A. ud-Doula, S. P. Owocki and R. H. Townsend, "Angular momentum loss and stellar spin-down in magnetic massive stars", *IAU Symposium*, ed. by K. G. Strassmeier, A. G. Kosovichev and J. E. Beckman, vol. 259, IAU Symposium, 2009 423–424, arXiv: 0812.2836 (cit. on p. 1).

[5] N. Langer, "Magnetic Fields in Stars: Origin and Impact", *IAU Symposium*, vol. 302, IAU Symposium, 2014 1–9, arXiv: 1312.2373 [astro-ph.SR] (cit. on p. 1).

[6] J. R. Hurley, O. R. Pols and C. A. Tout, *Comprehensive analytic formulae for stellar evolution as a function of mass and metallicity*, MNRAS **315** (2000) 543–569, eprint: astro-ph/0001295 (cit. on pp. 1, 3–5, 9, 14, 15).

[7] E. E. Salpeter, *The Luminosity Function and Stellar Evolution.*, ApJ **121** (1955) 161 (cit. on p. 3).

[8] N. Grevesse and A. J. Sauval, *Standard Solar Composition*, Space Sci. Rev. **85** (1998) 161–174 (cit. on p. 4).

[9] C. A. Tout et al., *Zero-age main-seqence radii and luminosities as analytic functions of mass and metallicity*, MNRAS **281** (1996) 257–262 (cit. on p. 4).

[10] P. J. Flower, *Transformations from Theoretical Hertzsprung-Russell Diagrams to Color-Magnitude Diagrams: Effective Temperatures, B-V Colors, and Bolometric Corrections*, ApJ **469** (1996) 355 (cit. on p. 4).

[11] E. B. Amôres and J. R. Lépine, *Models for Interstellar Extinction in the Galaxy*, AJ **130** (2005) 659–673 (cit. on pp. 4, 8).

[12] N. Castro et al., *The spectroscopic Hertzsprung-Russell diagram of Galactic massive stars*, A&A **570**, L13 (2014) L13, arXiv: 1410.3499 [astro-ph.SR] (cit. on p. 7).

[13] I. Brott et al., *Rotating massive main-sequence stars. I. Grids of evolutionary models and isochrones*, A&A **530**, A115 (2011) A115, arXiv: 1102.0530 [astro-ph.SR] (cit. on pp. 7, 9, 15).

[14] O. R. Pols et al., *Stellar evolution models for Z = 0.0001 to 0.03*, MNRAS **298** (1998) 525–536 (cit. on p. 9).

[15] H. Sana et al., *Binary Interaction Dominates the Evolution of Massive Stars*, Science **337** (2012) 444–, arXiv: 1207.6397 [astro-ph.SR] (cit. on p. 15).

[16] J. J. Paunzen E. Stütz C., *WEBDA A site Devoted to Stellar Clusters in the Galaxy and the Magellanic Clouds*, 2013, URL: http://www.univie.ac.at/webda/ (cit. on p. 16).